Monthly Notices
of the
ROYAL ASTRONOMICAL SOCIETY

MNRAS **502,** 2065–2073 (2021)
Advance Access publication 2021 January 22

doi:10.1093/mnras/stab187

A combined analysis of the H_0 late time direct measurements and the impact on the Dark Energy sector

Eleonora Di Valentino ★

Institute for Particle Physics Phenomenology, Department of Physics, Durham University, Durham, DH1 3LE, UK

Accepted 2021 January 19. Received 2021 January 19; in original form 2020 December 13

ABSTRACT

We combine 23 Hubble constant measurements based on Cepheids-SN Ia, TRGB-SN Ia, Miras-SN Ia, Masers, Tully Fisher, Surface Brightness Fluctuations, SN II, Time-delay Lensing, Standard Sirens and γ-ray Attenuation, obtaining our best *optimistic* H_0 estimate, that is $H_0 = 72.94 \pm 0.75$ km s^{-1} Mpc^{-1} at 68 per cent CL. This is in 5.9σ tension with the ΛCDM model, therefore we evaluate its impact on the extended Dark Energy cosmological models that can alleviate the tension. We find more than 4.9σ evidence for a phantom Dark Energy equation of state in the wCDM scenario, the cosmological constant ruled out at more than 3σ in a w_0w_a CDM model and more than 5.7σ evidence for a coupling between Dark Matter and Dark Energy in the IDE scenario. Finally, we check the robustness of our results; and we quote two additional combinations of the Hubble constant. The *ultra-conservative* estimate, $H_0 = 72.7 \pm 1.1$ km s^{-1} Mpc^{-1} at 68 per cent CL, is obtained removing the Cepheids-SN Ia and the Time-Delay Lensing based measurements, and confirms the evidence for new physics.

Key words: cosmic background radiation – cosmological parameters – cosmology: observations – dark energy.

1 INTRODUCTION

The ΛCDM model provides a wonderful explanation for most of the current cosmological probes. However, its validity is questioned by the robust tensions emerged between the early and the late time Universe measurements (see Di Valentino et al. 2020a,b for a recent overview). In particular, statistically significant is the long-standing Hubble constant tension at more than 4.4σ between the H_0 value estimated by Planck in Aghanim et al. (2020b) and that measured by the SH0ES collaboration in Riess et al. (2019; R19). The tension is made even more intriguing by the several early and late time cosmological probes (see Verde, Treu & Riess 2019; Riess 2019) in agreement, respectively, with Planck or R19, that make the systematic errors explanation more difficult, because biased always in the same direction.[1]

A gigantic effort is put into resolving the Hubble constant tension, and many cosmological scenarios, in alternative or extending the ΛCDM model, have been considered. We have, for example, early modifications of the expansion history, promising because, in principle, they could solve at the same time the H_0 tension and give a lower sound horizon $r_{\rm drag}$ at the drag epoch (Evslin, Sen & Ruchika 2018; Knox & Millea 2020) as preferred by the Baryon Acoustic Oscillations (BAO) data. The Early Dark Energy (Pettorino, Amendola & Wetterich 2013; Karwal & Kamionkowski 2016; Niedermann & Sloth 2019; Poulin et al. 2019; Akarsu et al. 2020; Sakstein & Trodden 2020; Ye & Piao 2020; Agrawal et al. 2019a; Lin et al. 2019; Berghaus & Karwal 2020; Smith, Poulin & Amin 2020; Lucca 2020; Braglia et al. 2020b) and extra relativistic species at recombination (Anchordoqui & Goldberg 2012; Jacques, Krauss & Lunardini 2013; Weinberg 2013; Anchordoqui, Goldberg & Steigman 2013; Carneiro et al. 2019; Paul et al. 2019; Di Valentino et al. 2016a; Green et al. 2019; Ferreira & Notari 2018; Gelmini, Kusenko & Takhistov 2019; Di Valentino et al. 2016b; Poulin et al. 2018; Baumann, Green & Wallisch 2016; Barenboim, Kinney & Park 2017; Zeng, Yeung & Chu 2019; Allahverdi et al. 2014; Braglia et al. 2020a) are the most famous models, but they can not increase the Hubble constant enough to solve the tension with R19 below 3σ (Arendse et al. 2020). The late time modifications of the expansion history, instead, have the capability of completely solving the Hubble tension with R19 within 1σ, but leave the sound horizon unaltered, introducing a tension with the BAO data. In this category, we find the phantom Dark Energy (Aghanim et al. 2020b; Yang et al. 2019c; Yang et al. 2019a; Di Valentino, Melchiorri & Silk 2020d; Vagnozzi 2020; Di Valentino, Mukherjee & Sen 2020c; Keeley et al. 2019; Joudaki et al. 2017; Alestas, Kazantzidis & Perivolaropoulos 2020) and the Phenomenologically Emergent Dark Energy (Li & Shafieloo 2019; Pan et al. 2020; Rezaei et al. 2020; Liu & Miao 2020; Li & Shafieloo 2020; Yang et al. 2020c). Another promising possibility is an interaction between the Dark Matter and the Dark Energy (IDE) models (Pettorino 2013; Wang et al. 2016; Kumar & Nunes 2016; Di Valentino, Melchiorri & Mena 2017; Kumar & Nunes 2017; Van De Bruck & Mifsud 2018; Yang et al. 2018b; Yang et al. 2018a; Yang et al. 2019b,d; Martinelli et al. 2019; Di Valentino et al. 2020e,f; Benevento, Hu & Raveri 2020; Gómez-Valent, Pettorino & Amendola 2020; Lucca & Hooper 2020; Yang et al. 2020a,b; Agrawal, Obied & Vafa 2019b; Anchordoqui et al. 2020a,b), that can solve completely the Hubble constant tension. In these models, there is a flux of energy between the dark matter and the dark energy, therefore, lowering the matter density, we can have a larger H_0 value

★ E-mail: eleonora.di-valentino@durham.ac.uk

[1] See also Dhawan, Jha & Leibundgut (2018) and Dhawan et al. (2020) for a discussion about the effect of possible systematic errors coming from dark energy model assumptions and the wavelength region of the observations.

for the geometrical degeneracy present in the CMB data (Di Valentino & Mena 2020).

In this paper, we combine, in an optimistic way, most of the late time measurements of the Hubble constant together, and we use this our best H_0 estimate to constrain some of the DE models that better solve the H_0 tension, namely wCDM, w_0w_aCDM, and IDE. Moreover, we test the robustness of our results using two additional Hubble constant estimates, that we will call *conservative* and *ultra-conservative*.

We introduce in Section 2, the data used in this paper and we explain the way we combine the different late time Hubble constant measurements; we present in Section 3, the Dark Energy models that we consider in this work; we describe in Section 4, the method used to analyse the cosmological parameters; we discuss in Section 5 the results we obtain; and we derive in Section 6, our conclusions.

2 OBSERVATIONAL DATA

To obtain our H_0 estimates, that we will use to constrain the cosmological parameters, we combine together most of the recent late time measurements (see Fig. 1 and Table 1) with a conservative approach, taking into account that not all measurements are fully independent even between techniques. In particular, we consider the measurements based on the following:

(i) Cepheids-SN Ia: We average the H_0 measurements from Riess et al. (2020), $73.2 \pm 1.3\,\mathrm{km\,s^{-1}\,Mpc^{-1}}$ at 68 per cent CL, from Breuval et al. (2020) with $H_0 = 73.0 \pm 2.7\,\mathrm{km\,s^{-1}\,Mpc^{-1}}$ at 68 per cent CL, from R19, $H_0 = 74.03 \pm 1.42\,\mathrm{km\,s^{-1}\,Mpc^{-1}}$ at 68 per cent CL, from Burns et al. (2018), $H_0 = 73.2 \pm 2.3\,\mathrm{km\,s^{-1}\,Mpc^{-1}}$ at 68 per cent CL, from Freedman et al. (2012), $H_0 = 74.3 \pm 2.1\,\mathrm{km\,s^{-1}\,Mpc^{-1}}$ at 68 per cent CL, and we use the smallest error bar of the group. [2] Therefore, we obtain $H_0 = 73.55 \pm 1.3\,\mathrm{km\,s^{-1}\,Mpc^{-1}}$ at 68 per cent CL for the measurements based on the Cepheids-SN Ia.

(ii) TRGB-SN Ia: We average the H_0 measurements from Soltis et al. (2020), $72.1 \pm 2.0\,\mathrm{km\,s^{-1}\,Mpc^{-1}}$ at 68 per cent CL, from Freedman et al. (2020), $H_0 = 69.6 \pm 0.8(stat) \pm 1.7(sys)\,\mathrm{km\,s^{-1}\,Mpc^{-1}}$ at 68 per cent CL, from Yuan et al. (2019), $H_0 = 72.4 \pm 2.0\,\mathrm{km\,s^{-1}\,Mpc^{-1}}$ at 68 per cent CL, from Jang & Lee (2017), $H_0 = 71.17 \pm 1.66(stat) \pm 1.87(sys)\,\mathrm{km\,s^{-1}\,Mpc^{-1}}$ at 68 per cent CL, and Reid et al. (2019), $H_0 = 71.1 \pm 1.9\,\mathrm{km\,s^{-1}\,Mpc^{-1}}$ at 68 per cent CL, and we use the smallest error bar of the group. Therefore, we obtain $H_0 = 71.27 \pm 1.88\,\mathrm{km\,s^{-1}\,Mpc^{-1}}$ at 68 per cent CL for the measurements based on the Tip of the Red Giant Branch.

(iii) Miras-SN Ia: We consider Huang et al. (2020), i.e. $H_0 = 73.3 \pm 4.0\,\mathrm{km\,s^{-1}\,Mpc^{-1}}$ at 68 per cent CL for measurement based on the Miras-SN Ia.

(iv) Masers: We consider Pesce et al. (2020), i.e. $H_0 = 73.9 \pm 3.0\,\mathrm{km\,s^{-1}\,Mpc^{-1}}$ at 68 per cent CL for the measurement based on the Masers.

(v) Tully Fisher: We average the H_0 measurements from Infrared Tully Fisher, Kourkchi et al. (2020), $H_0 = 76.0 \pm 1.1(stat) \pm 2.3(sys)\,\mathrm{km\,s^{-1}\,Mpc^{-1}}$ at 68 per cent CL, and from Baryonic Tully Fisher, Schombert et al. (2020), $H_0 = 75.1 \pm 2.3(stat) \pm 1.5(sys)\,\mathrm{km\,s^{-1}\,Mpc^{-1}}$ at 68 per cent CL, and we use the smallest error bar of the group. Therefore, we obtain $H_0 = 75.55 \pm 2.55\,\mathrm{km\,s^{-1}\,Mpc^{-1}}$ at 68 per cent CL for the measurements based on the Tully Fisher.

(vi) Surface-brightness fluctuations: We average the H_0 measurements from Blakeslee et al. (2021), $73.3 \pm 0.7 \pm 2.4\,\mathrm{km\,s^{-1}\,Mpc^{-1}}$ at 68 per cent CL, and from Khetan et al. (2020), $H_0 = 70.50 \pm 2.37(stat) \pm 3.38(sys)\,\mathrm{km\,s^{-1}\,Mpc^{-1}}$ at 68 per cent CL, that uses SN Ia, calibrated on the SBF distance. Therefore, we obtain $H_0 = 71.9 \pm 2.5\,\mathrm{km\,s^{-1}\,Mpc^{-1}}$ at 68 per cent CL for the measurement based on the Surface Brightness Fluctuations.

(vii) SN II: We consider de Jaeger et al. (2020), i.e. $H_0 = 75.8^{+5.2}_{-4.9}\,\mathrm{km\,s^{-1}\,Mpc^{-1}}$ at 68 per cent CL, for the measurement based on the SN II.

(viii) Time-delay lensing: We average the H_0 measurements from Wong et al. (2020) for six H0LiCOW lenses, $H_0 = 73.3^{+1.7}_{-1.8}\,\mathrm{km\,s^{-1}\,Mpc^{-1}}$ at 68 per cent CL, from Shajib et al. (2020) for STRIDES, $H_0 = 74.2^{+2.7}_{-3.0}\,\mathrm{km\,s^{-1}\,Mpc^{-1}}$ at 68 per cent CL, from Birrer et al. (2020) for TDCOSMO (six H0LiCOW and one STRIDES lenses), $H_0 = 74.5^{+5.6}_{-6.1}\,\mathrm{km\,s^{-1}\,Mpc^{-1}}$ at 68 per cent CL, and from Birrer et al. (2020) for TDCOSMO+SLACS (adding 33 SLACS lenses without time delays), $H_0 = 67.4^{+4.2}_{-3.2}\,\mathrm{km\,s^{-1}\,Mpc^{-1}}$ at 68 per cent CL, and we use the smallest error bar of the group. Therefore, we obtain $H_0 = 72.35 \pm 1.75\,\mathrm{km\,s^{-1}\,Mpc^{-1}}$ at 68 per cent CL for the measurements based on the Time-delay Lensing. [3]

(ix) Gravitational wave standard sirens: We consider Abbott et al. (2017), i.e. $H_0 = 70^{+12}_{-8}\,\mathrm{km\,s^{-1}\,Mpc^{-1}}$ at 68 per cent CL, for the measurement based on the Standard Sirens.

(x) γ-ray attenuation: we consider Domínguez et al. (2019), i.e. $H_0 = 67.4^{+6.0}_{-6.2}\,\mathrm{km\,s^{-1}\,Mpc^{-1}}$ at 68 per cent CL, for the measurement based on the γ-ray attenuation.

At this point, we consider a weighted average of the 10 estimates listed above, obtaining our best H_0 estimate, i.e. $H_0 = 72.94 \pm 0.75\,\mathrm{km\,s^{-1}\,Mpc^{-1}}$ at 68 per cent CL, in agreement with Verde et al. (2019). Computing the average over different measurements, made by different teams with different methods, can in principle ensure a more reliable H_0 estimate, perhaps cancelling possible biases, so we will call our best estimate *optimistic*. We notice here that we can safely add all the data sets together because all of them are in agreement within 2σ. However, there is some overlap between the data (i),(ii), and (iii), i.e. Cepheids, TRGB, and Miras, respectively, and SBF from Khetan et al. (2020) that use the same SN Ia ladders, and a more accurate analysis should account for their covariance. Therefore, in order to check the robustness and consistency of our optimistic estimate, we do a 'jackknife test' of the results, producing 10 averages with each leaving out a different data set, in Table 2, and 45 averages leaving out every combination of two, in Table 3. In particular, the exclusion of one measurement changes the H_0 estimate from the minimum mean value $H_0 = 72.63\,\mathrm{km\,s^{-1}\,Mpc^{-1}}$ to the maximum mean value $H_0 = 73.25\,\mathrm{km\,s^{-1}\,Mpc^{-1}}$ (see Table 2), while the exclusion of

[2] We compute the arithmetic average of these five measurements, i.e. $\frac{(73.2+73.0+74.03+73.2+74.3)}{5} = 73.55\,\mathrm{km\,s^{-1}\,Mpc^{-1}}$, but instead of quoting the error derived by the standard deviation (i.e. $0.52\,\mathrm{km\,s^{-1}\,Mpc^{-1}}$ in this case), we adopt a more conservative approach, preferring a larger error, i.e. the smallest error bar of the group, equal to $1.3\,\mathrm{km\,s^{-1}\,Mpc^{-1}}$. We repeat the same thing for the other cases. It should be noted here that we do not adopt a weighted average because of the correlation of the measurements, but in any case this would give a stronger bound, equal to $73.59 \pm 0.78\,\mathrm{km\,s^{-1}\,Mpc^{-1}}$.

[3] The results from Wong et al. (2020) for six H0LiCOW lenses and from Shajib et al. (2020) for STRIDES were obtained assuming the deflector mass density profiles by either a power law or stars (constant mass-to-light ratio) plus standard dark matter haloes, while the updated analysis in TDCOSMO IV does not rely on these assumptions on the radial density profiles, encodes the mass-sheet degeneracy in the inference and adds external lenses from the SLACS to provide quantitative constraints on the radial density profiles, providing a solid foundation of agnostic assumptions.

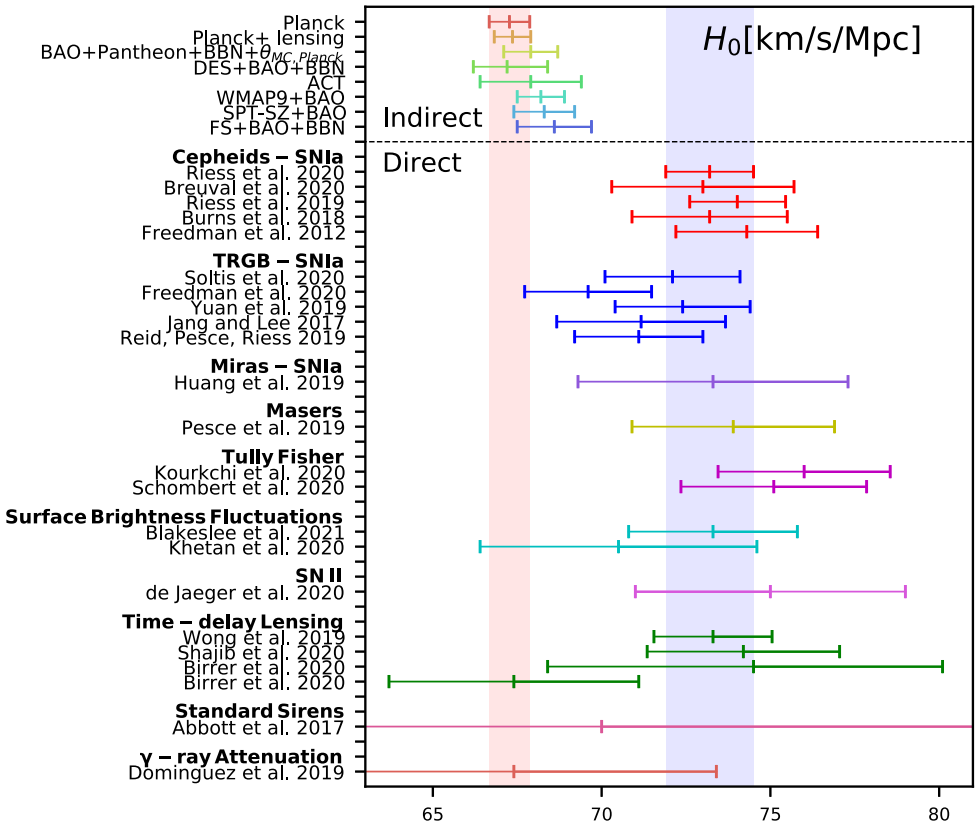

Figure 1. Some of the Hubble constant measurements present in the literature: see Table 1 for the values. Those averaged to obtain our H_0 estimates are instead listed in Section 4.

two measurements changes the H_0 estimate from minimum mean value $H_0 = 72.19\,\mathrm{km\,s^{-1}\,Mpc^{-1}}$ to the maximum mean value $H_0 = 73.51\,\mathrm{km\,s^{-1}\,Mpc^{-1}}$ (see Table 3). The robustness test shows that the exclusion of one or two of the listed measurements does not change quantitatively our conclusions on the DE models.

Regarding the correlation between the measurements (i),(ii), and (iii) (Cepheids, TRGB, and Miras, respectively) [4], we can see from Table 3 that considering only one of them per time does not change significantly our optimistic estimate. In particular, we find that removing (i) and (ii), we have $H_0 = 73.1 \pm 1.1\,\mathrm{km\,s^{-1}\,Mpc^{-1}}$ at 68 per cent CL, removing (i) and (iii), we have $H_0 = 72.59 \pm 0.95\,\mathrm{km\,s^{-1}\,Mpc^{-1}}$ at 68 per cent CL, and removing (ii) and (iii), we have $H_0 = 73.25 \pm 0.84\,\mathrm{km\,s^{-1}\,Mpc^{-1}}$ at 68 per cent CL. For this reason, we make use in the analysis of the DE models of an additional *conservative* estimate of H_0 from the Table 2 excluding one data set and taking the result with the largest error bar, i.e. $H_0 = 72.63 \pm 0.92\,\mathrm{km\,s^{-1}\,Mpc^{-1}}$ at 68 per cent CL without the Cepheids-SN Ia based measurement. And we consider an *ultra-conservative* estimate from the Table 3 excluding two data sets and taking the result with the largest error bar, i.e. $H_0 = 72.7 \pm 1.1\,\mathrm{km\,s^{-1}\,Mpc^{-1}}$ at 68 per cent CL, without also the Time-Delay Lensing based measurement.

The cosmological constraints on the parameters of the models we are analysing in this paper are then obtained, making use of the following data:

[4]The measurement from Khetan et al. (2020) based on SBF-SN has instead a relative larger uncertainty and is averaged with Blakeslee et al. (2021), that has the galaxies directly in the Hubble flow.

(i) Planck: For this data set, we consider the latest temperature and polarization Cosmic Microwave Background (CMB) power spectra data as measured by the final 2018 Planck legacy release (Aghanim et al. 2020a,b).

(ii) ACT+WMAP: We include this data set combination as in Ref. Aiola et al. (2020), as a crosscheck of the results, making use of the latest temperature and polarization CMB power spectra data as measured by ACT (Aiola et al. 2020), and combined with WMAP9 (Bennett et al. 2013) and a τ prior.

(iii) $optH_0$: We use a Gaussian prior on the Hubble constant as obtained by combining together, in an optimistic way, most of the late time measurement, i.e. $H_0 = 72.94 \pm 0.75\,\mathrm{km\,s^{-1}\,Mpc^{-1}}$ at 68 per cent CL. Moreover, we compare our results with those obtained using the conservative prior $H_0 = 72.63 \pm 0.92\,\mathrm{km\,s^{-1}\,Mpc^{-1}}$ at 68 per cent CL, i.e. $consH_0$, and the ultra-conservative prior $H_0 = 72.7 \pm 1.1\,\mathrm{km\,s^{-1}\,Mpc^{-1}}$ at 68 per cent CL, i.e. $ultraH_0$.

3 MODELS

Even if a ΛCDM model provides a beautiful description of the available cosmological data, we can not ignore the many H_0 measurements at late time providing a larger value for the Hubble constant. Our best optimistic estimate of $H_0 = 72.94 \pm 0.75\,\mathrm{km\,s^{-1}\,Mpc^{-1}}$ at 68 per cent CL is, in fact, at 5.9σ of disagreement with the Planck estimate in a ΛCDM model. Moreover, our H_0 estimate increases also the tension with the early time solutions, therefore making the late time solutions more appealing.

Actually, it is well known that BAO, combined with high-z SNe data, constrain the product $r_{\mathrm{drag}}H_0$, and combining them with either CMB or R19 leaves the other choice in tension, so the early time

Table 1. H_0 values at 68 per cent CL shown in Fig. 1, where we add in quadrature the systematic and statistic errors.

Data set	H_0 (km s^{-1} Mpc^{-1})
Planck Aghanim et al. (2020b)	67.27 ± 0.60
Planck+lensing Aghanim et al. (2020b)	67.36 ± 0.54
BAO+Pantheon+BBN+$\theta_{\rm MC,\ Planck}$ Aghanim et al. (2020b)	67.9 ± 0.8
DES+BAO+BBN Abbott et al. (2018)	$67.2^{+1.2}_{-1.0}$
ACT Aiola et al. (2020)	67.9 ± 1.5
WMAP9+BAO Addison et al. (2018)	68.2 ± 0.7
SPT-SZ+BAO Addison et al. (2018)	68.3 ± 0.9
FS+BAO+BBN Philcox et al. (2020)	68.6 ± 1.1
Riess et al. (2020)	73.2 ± 1.3
Breuval et al. (2020)	73.0 ± 2.7
R19	74.03 ± 1.42
Burns et al. (2018)	73.2 ± 2.3
Freedman et al. (2012)	74.3 ± 2.1
Soltis, Casertano & Riess (2020)	72.1 ± 2.0
Freedman et al. (2020)	69.6 ± 1.88
Yuan et al. (2019)	72.4 ± 2.0
Jang & Lee (2017)	71.17 ± 2.50
Reid, Pesce & Riess (2019)	71.1 ± 1.9
Huang et al. (2020)	73.3 ± 4.0
Pesce et al. (2020)	73.9 ± 3.0
Kourkchi et al. (2020)	76.00 ± 2.55
Schombert, McGaugh & Lelli (2020)	75.10 ± 2.75
Blakeslee et al. (2021)	73.3 ± 2.5
Khetan et al. (2020)	70.5 ± 4.1
de Jaeger et al. (2020)	$75.8^{+5.2}_{-4.9}$
Wong et al. (2020)	$73.3^{+1.7}_{-1.8}$
Shajib et al. (2020)	$74.2^{+2.7}_{-3.0}$
Birrer et al. (2020)	$74.5^{+5.6}_{-6.1}$
Birrer et al. (2020)	$67.4^{+4.2}_{-3.2}$
Abbott et al. (2017)	70^{+12}_{-8}
Domínguez et al. (2019)	$67.4^{+6.0}_{-6.2}$

Table 2. Robustness test of the results, excluding the measurement indicated in the last column.

H_0 mean	H_0 error	Excluded
72.62699	0.9233376	1
73.25471	0.8215147	2
72.92314	0.7664772	3
72.87175	0.7776620	4
72.68698	0.7878957	5
73.03983	0.7894195	6
72.87141	0.7612871	7
73.06965	0.8338738	8
72.95322	0.7549235	9
73.02211	0.7585800	10

solutions are preferred because they can modify both $r_{\rm drag}$ and H_0 in the right directions. However, we have chosen here to explore the most powerful extensions in solving the Hubble tension, without considering BAO and high-z SNe data. Actually, doing so may offer insight on some of the most famous DE models explored in the literature, focusing on just H_0 and neglecting for the moment additional data sets, that can bring further systematic errors in the general picture.

Table 3. Robustness test of the results, excluding the measurements indicated in the last two columns.

H_0 mean	H_0 error	Excluded	Excluded
73.05838	1.059989	1	2
72.58911	0.9489663	1	3
72.49379	0.9704452	1	4
72.18593	0.9905548	1	5
72.74182	0.9935880	1	6
72.51725	0.9391693	1	7
72.73386	1.086945	1	8
72.64958	0.9272990	1	9
72.74957	0.9341007	1	10
73.25271	0.8394086	2	3
73.20239	0.8541644	2	4
72.98889	0.8677809	2	5
73.41869	0.8698181	2	6
73.18552	0.8326054	2	7
73.51043	0.9304035	2	8
73.27682	0.8243009	2	9
73.36285	0.8290675	2	10
72.85492	0.7927890	3	4
72.66224	0.8036401	3	5
73.02929	0.8052573	3	6
72.85530	0.7754612	3	7
73.05918	0.8526064	3	8
72.94041	0.7687386	3	9
73.01174	0.7726005	3	10
72.59712	0.8165602	4	5
72.97585	0.8182568	4	6
72.80062	0.7870499	4	7
73.00013	0.7800242	4	9
72.96215	0.7840596	4	10
72.77377	0.8302036	5	6
72.60931	0.7976639	5	7
72.77266	0.8823864	5	8
72.70377	0.7903527	5	9
72.77669	0.7945514	5	10
72.97070	0.7992452	6	7
73.21607	0.8845285	6	8
73.05890	0.7918909	6	9
73.13590	0.7961143	6	10
72.99312	0.8454798	7	8
72.88815	0.7635028	7	9
72.95798	0.7672859	7	10
73.09115	0.8367882	8	9
73.17762	0.8417761	8	10
73.03960	0.7607720	9	10

Therefore in this work, we analyse three different models, famous for their ability to solve the Hubble constant tension within 2σ, so in good agreement with R19 and with our best optimistic estimate of H_0, as well as our conservative and ultra-conservative H_0 values.

First of all, we consider the wCDM model, where instead of a cosmological constant $w = -1$ there is a dark energy equation of state of the form $w = P/\rho$, where P and ρ are the dark energy pressure and dark energy density, respectively, and w is a free parameter time independent.

As a second scenario, we consider the w_0w_aCDM model, where there is a dark energy equation of state time dependent following the parametrization independently proposed by Chevallier & Polarski (2001) and Linder (2003), also known as CPL

$$w_x(a) = w_0 + w_a(1 - a). \quad (1)$$

Table 4. Flat priors on the cosmological parameters varied in this work.

Parameter	Prior
$\Omega_b h^2$	[0.005,0.1]
$\Omega_c h^2$	[0.001,0.99]
$100\theta_{MC}$	[0.5,10]
τ	[0.01,0.8]
n_S	[0.7,1.3]
$\log[10^{10}A_s]$	[1.7, 5.0]
w_0	[−3, 1]
w_a	[−3, 2]
ξ	[−1, 0]

In this parametrization, the dark energy equation-of-state parameter w_a gives the evolution of $w(a)$ with redshift, while w_0 gives the value of the dark energy equation of state today.

Finally, we consider an interacting dark energy scenario IDE, i.e. a class of models where the Dark Matter and Dark Energy continuity equations are described by Valiviita, Majerotto & Maartens (2008), del Campo, Herrera & Pavon (2009), Gavela et al. (2009, 2010), Honorez et al. (2010), and Di Valentino et al. (2020e,f)

$$\dot{\rho}_c + 3\mathcal{H}\rho_c = Q\,, \tag{2}$$

$$\dot{\rho}_x + 3\mathcal{H}(1+w)\rho_x = -Q\,. \tag{3}$$

In these equations, the dot refer to the derivative with respect to the conformal time τ, ρ_c is the dark matter energy density, $\mathcal{H}$ is the conformal expansion rate of the universe, ρ_x is dark-energy density. In our analysis, we assume a constant dark energy equation of state $w = -0.999$ and a coupling function Q given by

$$Q = \xi\mathcal{H}\rho_x\,, \tag{4}$$

where ξ is a negative dimensionless parameter, describing the coupling between the dark matter and the dark energy fluids.

4 METHODOLOGY

We analyse three different baseline models, namely wCDM, w_0w_aCDM, and IDE described in Section 3. The common six cosmological parameters of the models considered in this work are the baryon energy density $\Omega_b h^2$, the cold dark matter energy density $\Omega_c h^2$, the ratio between the sound horizon and the angular diameter distance at decoupling θ_{MC}, the reionization optical depth τ, the amplitude of the scalar primordial power spectrum A_s, the spectral index n_s. The specific parameters of the cosmological scenario analysed with the data, are instead the constant Dark Energy equation of state w for the wCDM model, the two parameters of the redshift dependent Dark Energy equation of state w_0, w_a for the w_0w_a CDM model, and the dimensionless coupling ξ for the IDE model. We adopt on the parameters the flat priors listed in Table 4.

For the data analysis, we make use of the publicly available MCMC code `cosmomc` (Lewis & Bridle 2002; see http://cosmologist.info/cosmomc/), also modified to implement the IDE model. This code implements an efficient sampling of the posterior distribution using the fast/slow parameter decorrelations (Lewis 2013) and makes use of a convergence diagnostic based on the Gelman–Rubin statistics (Gelman & Rubin 1992).

5 RESULTS

We present in Table 5 the 68 per cent CL constraints on the cosmological parameters of the DE models explored in this work (wCDM, w_0w_a CDM, and IDE) obtained combining Planck with our optimistic H_0 prior, i.e. $H_0 = 72.94 \pm 0.75\,\mathrm{km\,s^{-1}\,Mpc^{-1}}$ at 68 per cent CL, presented in Section 4. We show, instead, in Table 7 the bounds on the cosmological models wCDM and w_0w_aCDM we find combining ACT+WMAP and our optimistic H_0 prior. We remind here that we can combine these measurements safely because in good agreement with our optimistic H_0 prior within these cosmological scenarios.

The wCDM cosmological constraints are reported in the first two columns of Tables 5 and 7. We can see a good agreement between Planck and ACT+WMAP, but with Planck preferring a larger Hubble constant and a more phantom dark energy equation of state than ACT+WMAP. In particular, while $H_0 > 82.5\,\mathrm{km\,s^{-1}\,Mpc^{-1}}$ at 68 per cent CL for Planck, therefore in agreement with our optimistic H_0 estimate at 95 per cent CL, ACT+WMAP finds $H_0 = 72^{+9}_{-20}\,\mathrm{km\,s^{-1}\,Mpc^{-1}}$ at 68 per cent CL, i.e. in agreement within 1σ with our $optH_0$ prior. Combining these CMB data sets with our optimistic H_0, we find instead a perfect agreement between the two data set combinations, Planck based and ACT based, removing the main differences. Planck+$optH_0$ gives, in fact, an

Table 5. 68 per cent CL constraints for the wCDM, w_0w_aCDM, and IDE scenarios explored in this work, for Planck and Planck+$optH_0$.

Parameters	wCDM Planck	wCDM Planck + $optH_0$	w_0w_a CDM Planck	w_0w_aCDM Planck + $optH_0$	IDE Planck	IDE Planck + $optH_0$
$\Omega_b h^2$	0.02240 ± 0.00015	0.02238 ± 0.00015	0.02240 ± 0.00015	0.02240 ± 0.00015	0.02239 ± 0.000015	0.02238 ± 0.000014
$\Omega_c h^2$	0.1199 ± 0.0014	$0.1201^{+0.0014}_{-0.0015}$	0.1198 ± 0.0014	0.1198 ± 0.0014	<0.0634	$0.046^{+0.014}_{-0.012}$
$100\theta_{MC}$	1.04093 ± 0.00031	1.04091 ± 0.00031	1.04094 ± 0.00031	1.04092 ± 0.00031	$1.0458^{+0.0033}_{-0.0021}$	$1.0458^{+0.0009}_{-0.0012}$
τ	0.0540 ± 0.0079	0.0536 ± 0.0080	$0.0541^{+0.0073}_{-0.0084}$	0.0544 ± 0.0081	0.0541 ± 0.0076	0.0540 ± 0.0076
n_s	0.9654 ± 0.0044	$0.9649^{+0.0052}_{-0.0046}$	0.9657 ± 0.0043	0.9655 ± 0.0043	0.9655 ± 0.0043	0.9652 ± 0.0042
$\ln(10^{10}A_s)$	3.044 ± 0.016	3.043 ± 0.016	3.044 ± 0.017	3.044 ± 0.017	3.044 ± 0.0016	3.044 ± 0.0016
ξ	0	0	0	0	$-0.54^{+0.12}_{-0.28}$	$-0.57^{+0.10}_{-0.09}$
w_0	$-1.58^{+0.16}_{-0.35}$	$-1.187^{+0.038}_{-0.030}$	$-1.25^{+0.40}_{-0.56}$	$-0.83^{+0.29}_{-0.17}$	-0.999	-0.999
w_a	0	0	<-0.646	<-1.05	0	0
H_0 ($\mathrm{km\,s^{-1}\,Mpc^{-1}}$)	>82.5	72.97 ± 0.75	>79.5	72.96 ± 0.74	$72.8^{+3.0}_{-1.5}$	73.04 ± 0.74
S_8	$0.778^{+0.023}_{-0.036}$	0.817 ± 0.015	$0.786^{+0.026}_{-0.044}$	0.819 ± 0.015	$1.30^{+0.17}_{-0.44}$	$1.24^{+0.09}_{-0.18}$
r_d (Mpc)	147.08 ± 0.30	147.05 ± 0.31	147.10 ± 0.30	147.11 ± 0.30	147.08 ± 0.30	147.06 ± 0.29

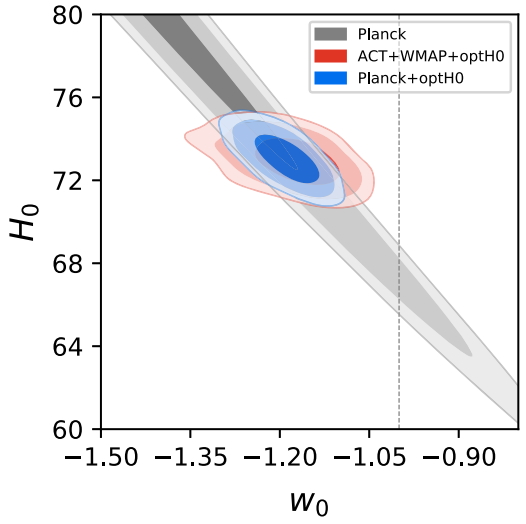

Figure 2. 68, 95, and 99 per cent contour plots for the wCDM model in the plane (w, H_0). We can see the evidence for a phantom Dark Energy equation of state at more than 5σ for Planck+$optH_0$, and at more than 3σ for ACT+WMAP+$optH_0$.

evidence for a phantom Dark Energy equation of state at more than 4.9σ, i.e. $w = -1.187^{+0.038}_{-0.030}$ at 68 per cent CL, in agreement with ACT+WMAP+$optH_0$, that finds $w = -1.172^{+0.052}_{-0.040}$ at 68 per cent CL, ruling out the cosmological constant at more than 3.3σ. The correlation between w and H_0 can be seen in Fig. 2, as well as the strong evidence for a phantom dark energy coming from both, Planck+$optH_0$ and ACT+WMAP+$optH_0$. To test the robustness of our results, we make use of our conservative H_0 estimate $H_0 = 72.63 \pm 0.92\,\mathrm{km\,s^{-1}\,Mpc^{-1}}$ at 68 per cent CL, obtaining $w = -1.178^{+0.040}_{-0.033}$ at 68 per cent CL for Planck+$consH_0$, corresponding to the first column of Table 6, and $w = -1.163^{+0.053}_{-0.043}$ at 68 per cent CL for ACT+WMAP+$consH_0$, corresponding to the first column of Table 8. Additionally, if we move to our ultra-conservative H_0 estimate, $H_0 = 72.7 \pm 1.1\,\mathrm{km\,s^{-1}\,Mpc^{-1}}$ at 68 per cent CL, we obtain $w = -1.182^{+0.045}_{-0.038}$ at 68 per cent CL for Planck+$ultraH_0$, corresponding to the second column of Table 6, and $w = -1.165^{+0.056}_{-0.046}$ at 68 per cent CL for ACT+WMAP+$ultraH_0$, corresponding to the second column of Table 8. Therefore, we are ruling out the cosmological constant at more than 3σ in all the cases.

The constraints on the cosmological parameters of the w_0w_aCDM scenario are shown in the columns 3 and 4 of Tables 5 and 7. Also in this case, we have a good agreement between Planck and ACT+WMAP, with Planck preferring a larger H_0 value than ACT+WMAP. In particular, Planck gives $H_0 > 79.5\,\mathrm{km\,s^{-1}\,Mpc^{-1}}$ at 68 per cent CL, in agreement with our H_0 estimates at 95 per cent CL, while ACT+WMAP prefers $H_0 = 70^{+10}_{-20}\,\mathrm{km\,s^{-1}\,Mpc^{-1}}$ at 68 per cent CL, in agreement within 1σ with our $optH_0$ prior. If we now combine these two data set combinations with our optimistic H_0 estimate, Planck+$optH_0$ gives $w_0 = -0.83^{+0.29}_{-0.17}$ and $w_a < -1.05$ at 68 per cent CL, and ACT+WMAP+$optH_0$ finds $w_0 = -1.07 \pm 0.33$ and $w_a < 0.327$ at 68 per cent CL. In Fig. 3, we can see as both, Planck+$optH_0$ and ACT+WMAP+$optH_0$, are ruling out a cosmological constant, i.e. the point ($w_0 = -1$, $w_a = 0$), at more than three standard deviations. To check the robustness of our constraints, we make use of our conservative H_0 estimate obtaining $w_0 = -0.82^{+0.29}_{-0.17}$ and $w_a < -1.04$ at 68 per cent CL for Planck+$consH_0$, in Table 6, and $w_0 = -1.06^{+0.38}_{-0.34}$ and $w_a =$

Table 6. 68 per cent CL constraints for the wCDM, w_0w_aCDM, and IDE scenarios explored in this work, for Planck+$consH_0$ and Planck+$ultraH_0$.

Parameters	wCDM Planck + $consH_0$	wCDM Planck + $ultraH_0$	w_0w_aCDM Planck + $consH_0$	w_0w_aCDM Planck + $ultraH_0$	IDE Planck + $consH_0$	IDE Planck + $ultraH_0$
ξ	0	0	0	0	-0.55 ± 0.11	-0.56 ± 0.12
w_0	$-1.178^{+0.040}_{-0.033}$	$-1.182^{+0.045}_{-0.038}$	$-0.82^{+0.29}_{-0.17}$	$-0.82^{+0.29}_{-0.17}$	-0.999	-0.999
w_a	0	0	<-1.04	<-1.05	0	0
H_0 ($\mathrm{km\,s^{-1}\,Mpc^{-1}}$)	72.69 ± 0.91	72.8 ± 1.1	72.67 ± 0.92	72.8 ± 1.1	72.79 ± 0.91	72.9 ± 1.1
S_8	0.818 ± 0.015	0.818 ± 0.015	0.820 ± 0.015	0.820 ± 0.015	$1.21^{+0.09}_{-0.19}$	$1.23^{+0.10}_{-0.22}$
r_d (Mpc)	147.05 ± 0.30	147.05 ± 0.30	147.11 ± 0.30	147.11 ± 0.31	147.06 ± 0.29	147.06 ± 0.29

Table 7. 68 per cent CL constraints for the wCDM and w_0w_aCDM scenarios explored in this work, for ACT+WMAP and ACT+WMAP+$optH_0$.

Parameters	wCDM ACT + WMAP	wCDM ACT + WMAP + $optH_0$	w_0w_aCDM ACT + WMAP	w_0w_aCDM ACT + WMAP + $optH_0$
$\Omega_b h^2$	0.02238 ± 0.00020	0.02239 ± 0.00020	0.02238 ± 0.00021	0.02237 ± 0.00021
$\Omega_c h^2$	0.1202 ± 0.0027	0.1200 ± 0.0025	0.1203 ± 0.0028	$0.1203^{+0.0026}_{-0.0029}$
$100\theta_{MC}$	1.04167 ± 0.00064	1.04172 ± 0.00066	1.04168 ± 0.00065	$1.04171^{+0.00070}_{-0.00064}$
τ	0.062 ± 0.013	0.062 ± 0.013	0.061 ± 0.013	0.061 ± 0.013
n_s	0.9727 ± 0.0063	0.9730 ± 0.0059	0.9727 ± 0.0064	0.9725 ± 0.0062
$\ln(10^{10}A_s)$	3.067 ± 0.024	3.066 ± 0.024	3.065 ± 0.024	3.064 ± 0.024
w_0	$-1.12^{+0.56}_{-0.32}$	$-1.172^{+0.052}_{-0.040}$	$-0.83^{+0.69}_{-0.83}$	-1.07 ± 0.33
w_a	0	0	<-0.158	<0.327
H_0 ($\mathrm{km\,s^{-1}\,Mpc^{-1}}$)	72^{+9}_{-20}	72.87 ± 0.73	70^{+10}_{-20}	72.90 ± 0.75
S_8	$0.828^{+0.049}_{-0.043}$	0.827 ± 0.025	0.836 ± 0.051	0.827 ± 0.028
r_d (Mpc)	147.03 ± 0.63	147.07 ± 0.61	147.00 ± 0.66	$147.02^{+0.68}_{-0.61}$

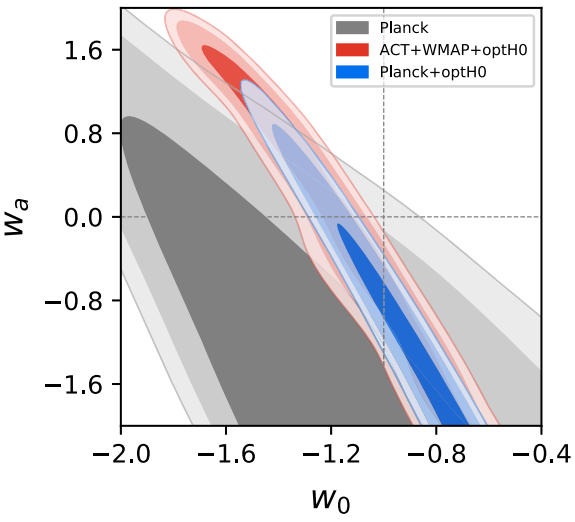

Figure 3. 68, 95, and 99 per cent contour plots for the w_0w_aCDM model in the plane (w, w_a). We can see that both the data set combinations, Planck+*optH*$_0$ and ACT+WMAP+*optH*$_0$, are ruling out a cosmological constant, i.e. the point ($w_0 = -1$, $w_a = 0$), at many standard deviations with a large statistical significance.

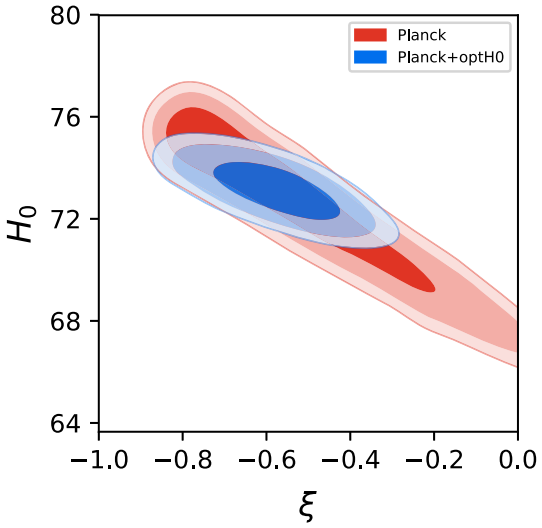

Figure 4. 68, 95, and 99 per cent contour plots for the IDE model in the plane (ξ, H_0). We see for Planck+*optH*$_0$ a strong evidence for an interaction between the dark energy and the dark matter at more than 6σ.

$-0.5^{+1.9}_{-1.3}$ at 68 per cent CL for ACT+WMAP+*consH*$_0$ in Table 8. Moreover, for our ultra-conservative H_0 estimate, we have $w_0 = -0.82^{+0.29}_{-0.17}$ and $w_a < -1.05$ at 68 per cent CL for Planck+*ultraH*$_0$ (Table 6) and $w_0 = -1.05^{+0.39}_{-0.33}$ and $w_a = -0.6^{+1.9}_{-1.3}$ at 68 per cent CL for ACT+WMAP+*ultraH*$_0$ (Table 8). In all the cases, we are ruling out the cosmological constant in the plane (w_0, w_a) at more than 3σ.

The constraints for the IDE scenario are shown in the columns 5 and 6 of Table 5. In this model, we have a suspicious evidence for a coupling between the dark matter and the dark energy, possibly due to the correlation of the parameters, as shown in Di Valentino & Mena (2020), for Planck alone. In particular, for this model, Planck gives $H_0 = 72.8^{+3.0}_{-1.5}$ km s^{-1} Mpc^{-1} at 68 per cent CL, in agreement with our optimistic H_0 estimate at 68 per cent CL. If we now combine this data set with our optimistic H_0 prior, we break the degeneracy between the parameters, obtaining for Planck+*optH*$_0$ a coupling $\xi = -0.57^{+0.10}_{-0.09}$ at 68 per cent CL, i.e. a strong evidence for an interaction between the dark energy and the dark matter at more than 5.7σ, as we can see also in Fig. 4. It is worthwhile to note that making use of the our conservative H_0 prior, we have $\xi = -0.55 \pm 0.11$ at 68 per cent CL, and of our ultra-conservative H_0 prior, we have $\xi = -0.56 \pm 0.12$ at 68 per cent CL, reducing the evidence for the coupling at 5σ and 4.7σ, respectively, corresponding to the last two columns of Table 6.

6 CONCLUSIONS

In this paper, we study the impact of the Hubble Constant H_0 late time measurements on the Dark Energy sector. First, we combine some of the latest H_0 measurements, testing the consistency and robustness of the results excluding one, or two, different measurements per time. Then, we define our best optimistic H_0 estimate, that is $H_0 = 72.94 \pm 0.75$ km s^{-1} Mpc^{-1} at 68 per cent CL, obtained averaging over different measurements, made by different teams with different methods, in order to guarantee a more reliable H_0 estimate, possibly cancelling likely biases. Finally, we evaluate the impact of this H_0 prior on extended Dark Energy cosmologies, in particular wCDM, with a constant dark energy equation of state, w_0w_aCDM, with a varying with redshift dark energy equation of state, and an IDE scenario, where there is an interaction between dark matter and dark energy.

We find for wCDM that a combination of Planck+*optH*$_0$ gives an evidence for a phantom Dark Energy equation of state at more than 4.9σ, i.e. $w = -1.187^{+0.038}_{-0.030}$ at 68 per cent CL, and this result is supported by ACT+WMAP+*optH*$_0$ that finds $w < -1$ at more than 3σ, i.e. $w = -1.172^{+0.052}_{-0.040}$ at 68 per cent CL.

We find for w_0w_aCDM that both the data set combinations, Planck+*optH*$_0$ and ACT+WMAP+*optH*$_0$, are ruling out a cosmological constant, i.e. the point ($w_0 = -1$, $w_a = 0$), at more than 3σ.

Table 8. 68 per cent CL constraints for the wCDM and w_0w_aCDM scenarios explored in this work, for ACT+WMAP+*consH*$_0$ and ACT+WMAP+*ultraH*$_0$.

Parameters	wCDM ACT + WMAP + *consH*$_0$	wCDM ACT + WMAP + *ultraH*$_0$	w_0w_aCDM ACT + WMAP + *consH*$_0$	w_0w_aCDM ACT + WMAP + *ultraH*$_0$
w_0	$-1.163^{+0.053}_{-0.043}$	$-1.165^{+0.056}_{-0.046}$	$-1.06^{+0.38}_{-0.34}$	$-1.05^{+0.39}_{-0.33}$
w_a	0	0	$-0.5^{+1.9}_{-1.3}$	$-0.6^{+1.9}_{-1.3}$
H_0 (km s^{-1} Mpc^{-1})	72.58 ± 0.88	72.6 ± 1.1	72.58 ± 0.92	72.6 ± 1.1
S_8	0.828 ± 0.026	0.828 ± 0.026	0.829 ± 0.028	0.828 ± 0.028
r_d (Mpc)	147.06 ± 0.61	147.07 ± 0.61	$147.01^{+0.68}_{-0.62}$	147.01 ± 0.67

We see for Planck+*optH*$_0$ a coupling $\xi = -0.57^{+0.10}_{-0.09}$ at 68 per cent CL, i.e. a strong evidence for an interaction between the dark energy and the dark matter at more than 5.7σ.

Finally, if we check the robustness of our conclusions making use of a conservative or ultra-conservative H_0 priors, we find that these results are confirmed. We remind here that these DE models are in any case in tension with BAO and high-z SNe data.

ACKNOWLEDGEMENTS

The author thanks Adam Riess for explanations regarding differences in Hubble constant measurements and Simon Birrer for those based on the Time-delay Lensing. In addition, the author thanks Alessandro Melchiorri and Olga Mena for useful discussions. The author acknowledges the support of the Addison-Wheeler Fellowship awarded by the Institute of Advanced Study, Durham University.

DATA AVAILABILITY

We used current publicly available cosmological probes, as listed in the section 'Observational Data'.

REFERENCES

Abbott B. P. et al., 2017, Nature, 551, 85
Abbott T. et al., 2018, MNRAS, 480, 3879
Addison G., Watts D., Bennett C., Halpern M., Hinshaw G., Weiland J., 2018, ApJ, 853, 119
Aghanim N. et al., 2020a, A&A, 641, A5
Aghanim N. et al., 2020b, A&A, 641, A6
Agrawal P., Cyr-Racine F.-Y., Pinner D., Randall L., 2019a, preprint (arXiv:1904.01016)
Agrawal P., Obied G., Vafa C., 2019b, preprint (arXiv:1906.08261)
Aiola S. et al., 2020, JCAP, 12, 33
Akarsu Ö., Barrow J. D., Escamilla L. A., Vazquez J. A., 2020, Phys. Rev. D, 101, 063528
Alestas G., Kazantzidis L., Perivolaropoulos L., 2020, Phys. Rev. D, 101, 123516
Allahverdi R., Cicoli M., Dutta B., Sinha K., 2014, JCAP, 10, 002
Anchordoqui L. A., Goldberg H., 2012, Phys. Rev. Lett., 108, 081805
Anchordoqui L. A., Goldberg H., Steigman G., 2013, Phys. Lett. B, 718, 1162
Anchordoqui L. A., Antoniadis I., Lüst D., Soriano J. F., 2020a, preprint (arXiv:2005.10075)
Anchordoqui L. A., Antoniadis I., Lüst D., Soriano J. F., Taylor T. R., 2020b, Phys. Rev. D, 101, 083532
Arendse N. et al., 2020, A&A, 639, A57
Barenboim G., Kinney W. H., Park W.-I., 2017, Eur. Phys. J. C, 77, 590
Baumann D., Green D., Wallisch B., 2016, Phys. Rev. Lett., 117, 171301
Benevento G., Hu W., Raveri M., 2020, Phys. Rev. D, 101, 103517
Bennett C. et al., 2013, ApJS, 208, 20
Berghaus K. V., Karwal T., 2020, Phys. Rev. D, 101, 083537
Birrer S. et al., 2020, A&A, 643, A165
Blakeslee J. P., Jensen J. B., Ma C.-P., Milne P. A., Greene J. E., 2021, preprint (arXiv:2101.02221)
Braglia M., Ballardini M., Emond W. T., Finelli F., Gumrukcuoglu A. E., Koyama K., Paoletti D., 2020a, Phys. Rev. D, 102, 023529
Braglia M., Emond W. T., Finelli F., Gumrukcuoglu A. E., Koyama K., 2020b, Phys. Rev. D, 102, 083513
Breuval L. et al., 2020, A&A, 643, A115
Burns C. R. et al., 2018, ApJ, 869, 56
Carneiro S., de Holanda P. C., Pigozzo C., Sobreira F., 2019, Phys. Rev., D100, 023505
Chevallier M., Polarski D., 2001, Int. J. Mod. Phys., D10, 213
del Campo S., Herrera R., Pavon D., 2009, JCAP, 01, 020
de Jaeger T., Stahl B., Zheng W., Filippenko A., Riess A., Galbany L., 2020, MNRAS, 496, 3402
Dhawan S., Jha S. W., Leibundgut B., 2018, A&A, 609, A72
Dhawan S., Brout D., Scolnic D., Goobar A., Riess A., Miranda V., 2020, ApJ, 894, 54
Di Valentino E. et al., 2020a, preprint (arXiv:2008.11284)
Di Valentino E. et al., 2020b, preprint (arXiv:2008.11285)
Di Valentino E., Mena O., 2020, Mon.Not.Roy.Astron.Soc., 500, L22
Di Valentino E., Giusarma E., Mena O., Melchiorri A., Silk J., 2016a, Phys. Rev., D93, 083527
Di Valentino E., Giusarma E., Lattanzi M., Mena O., Melchiorri A., Silk J., 2016b, Phys. Lett., B752, 182
Di Valentino E., Melchiorri A., Mena O., 2017, Phys. Rev., D96, 043503
Di Valentino E., Mukherjee A., Sen A. A., 2020c, preprint (arXiv:2005.12587)
Di Valentino E., Melchiorri A., Silk J., 2020d, JCAP, 01, 013
Di Valentino E., Melchiorri A., Mena O., Vagnozzi S., 2020e, Phys. Dark Univ., 30, 100666
Di Valentino E., Melchiorri A., Mena O., Vagnozzi S., 2020f, Phys. Rev. D, 101, 063502
Domínguez A. et al., 2019, ApJ, 885, 9
Evslin J., Sen A. A., Ruchika, 2018, Phys. Rev. D, 97, 103511
Ferreira R. Z., Notari A., 2018, Phys. Rev. Lett., 120, 191301
Freedman W. L., Madore B. F., Scowcroft V., Burns C., Monson A., Persson S. E., Seibert M., Rigby J., 2012, AJ, 758, 24
Freedman W. L. et al., 2020, ApJ, 891, 33
Gavela M., Hernandez D., Lopez Honorez L., Mena O., Rigolin S., 2009, JCAP, 07, 034
Gavela M., Lopez Honorez L., Mena O., Rigolin S., 2010, JCAP, 11, 044
Gelman A., Rubin D. B., 1992, Stat. Sci., 7, 457
Gelmini G. B., Kusenko A., Takhistov V., 2019, preprint (arXiv:1906.10136)
Gómez-Valent A., Pettorino V., Amendola L., 2020, Phys. Rev. D, 101, 123513
Green D. et al., 2019, BAAS, 51, 159
Honorez L. L., Reid B. A., Mena O., Verde L., Jimenez R., 2010, JCAP, 2010, 029
Huang C. D. et al., 2020, ApJ, 889, 5
Jacques T. D., Krauss L. M., Lunardini C., 2013, Phys. Rev. D, 87, 083515
Jang I. S., Lee M. G., 2017, ApJ, 836, 74
Joudaki S. et al., 2017, MNRAS, 471, 1259
Karwal T., Kamionkowski M., 2016, Phys. Rev. D, 94, 103523
Keeley R. E., Joudaki S., Kaplinghat M., Kirkby D., 2019, JCAP, 12, 035
Khetan N. et al., 2020, preprint (arXiv:2008.07754)
Knox L., Millea M., 2020, Phys. Rev. D, 101, 043533
Kourkchi E., Tully R. B., Anand G. S., Courtois H. M., Dupuy A., Neill J. D., Rizzi L., Seibert M., 2020, ApJ, 896, 3
Kumar S., Nunes R. C., 2016, Phys. Rev., D94, 123511
Kumar S., Nunes R. C., 2017, Phys. Rev., D96, 103511
Lewis A., 2013, Phys. Rev. D, 87, 103529
Lewis A., Bridle S., 2002, Phys. Rev. D, 66, 103511
Li X., Shafieloo A., 2019, ApJ, 883, L3
Li X., Shafieloo A., 2020, ApJ, 902, 58
Linder E. V., 2003, Phys. Rev. Lett., 90, 091301
Lin M.-X., Benevento G., Hu W., Raveri M., 2019, Phys. Rev. D, 100, 063542
Liu Z., Miao H., 2020, Int. J. Mod. Phys. D, 29, 2050088
Lucca M., 2020, Phys. Lett. B, 810, 135791
Lucca M., Hooper D. C., 2020, Phys. Rev. D, 102, 123502
Martinelli M., Hogg N. B., Peirone S., Bruni M., Wands D., 2019, MNRAS, 488, 3423
Niedermann F., Sloth M. S., 2019, preprint (arXiv:1910.10739)
Pan S., Yang W., Di Valentino E., Shafieloo A., Chakraborty S., 2020, JCAP, 06, 062
Paul A., Ghoshal A., Chatterjee A., Pal S., 2019, Eur. Phys. J., C79, 818
Pesce D. et al., 2020, ApJ, 891, L1
Pettorino V., 2013, Phys. Rev. D, 88, 063519
Pettorino V., Amendola L., Wetterich C., 2013, Phys. Rev. D, 87, 083009
Philcox O. H., Ivanov M. M., Simonović M., Zaldarriaga M., 2020, JCAP, 05, 032

Poulin V., Smith T. L., Grin D., Karwal T., Kamionkowski M., 2018, Phys. Rev. D, 98, 083525
Poulin V., Smith T. L., Karwal T., Kamionkowski M., 2019, Phys. Rev. Lett., 122, 221301
Reid M., Pesce D., Riess A., 2019, ApJ, 886, L27
Rezaei M., Naderi T., Malekjani M., Mehrabi A., 2020, Eur. Phys. J. C, 80, 374
Riess A. G., 2019, Nature Rev. Phys., 2, 10
Riess A. G., Casertano S., Yuan W., Macri L. M., Scolnic D., 2019, ApJ, 876, 85
Riess A. G., Casertano S., Yuan W., Bowers J. B., Macri L., Zinn J. C., Scolnic D., 2020, preprint (arXiv:2012.08534)
Sakstein J., Trodden M., 2020, Phys. Rev. Lett., 124, 161301
Schombert J., McGaugh S., Lelli F., 2020, AJ, 160, 71
Shajib A. et al., 2020, MNRAS, 494, 6072
Smith T. L., Poulin V., Amin M. A., 2020, Phys. Rev. D, 101, 063523
Soltis J., Casertano S., Riess A. G., 2020, preprint (arXiv:2012.09196)
Vagnozzi S., 2020, Phys. Rev. D, 102, 023518
Valiviita J., Majerotto E., Maartens R., 2008, JCAP, 07, 020
Van De Bruck C., Mifsud J., 2018, Phys. Rev. D, 97, 023506
Verde L., Treu T., Riess A., 2019, Nature Astron., 3, 891
Wang B., Abdalla E., Atrio-Barandela F., Pavon D., 2016, Rept. Prog. Phys., 79, 096901
Weinberg S., 2013, Phys. Rev. Lett., 110, 241301
Wong K. C. et al., 2020, MNRAS, 498, 1420
Yang W., Mukherjee A., Di Valentino E., Pan S., 2018a, Phys. Rev., D98, 123527
Yang W., Pan S., Di Valentino E., Nunes R. C., Vagnozzi S., Mota D. F., 2018b, JCAP, 1809, 019
Yang W., Pan S., Di Valentino E., Saridakis E. N., 2019a, Universe, 5, 219
Yang W., Pan S., Xu L., Mota D. F., 2019b, MNRAS, 482, 1858
Yang W., Pan S., Di Valentino E., Saridakis E. N., Chakraborty S., 2019c, Phys. Rev., D99, 043543
Yang W., Mena O., Pan S., Di Valentino E., 2019d, Phys. Rev., D100, 083509
Yang W., Pan S., Nunes R. C., Mota D. F., 2020a, JCAP, 04, 008
Yang W., Di Valentino E., Mena O., Pan S., Nunes R. C., 2020b, Phys. Rev. D, 101, 083509
Yang W., Di Valentino E., Mena O., Pan S., 2020c, Phys. Rev. D, 102, 023535
Ye G., Piao Y.-S., 2020, Phys. Rev. D, 101, 083507
Yuan W., Riess A. G., Macri L. M., Casertano S., Scolnic D., 2019, ApJ, 886, 61
Zeng Z., Yeung S., Chu M.-C., 2019, JCAP, 03, 015

This paper has been typeset from a TEX/LATEX file prepared by the author.